

M. Koch-Müller · P. Dera · Y. Fei · H. Hellwig
Z. Liu · J. Van Orman · R. Wirth

Polymorphic phase transition in Superhydrous Phase B

Received: 15 October 2004 / Accepted: 24 March 2005 / Published online: 21 July 2005
© Springer-Verlag 2005

Abstract We synthesized superhydrous phase B (shy-B) at 22 GPa and two different temperatures: 1200°C (LT) and 1400°C (HT) using a multi-anvil apparatus. The samples were investigated by transmission electron microscopy (TEM), single crystal X-ray diffraction, Raman and IR spectroscopy. The IR spectra were collected on polycrystalline thin-films and single crystals using synchrotron radiation, as well as a conventional IR source at ambient conditions and in situ at various pressures (up to 15 GPa) and temperatures (down to –180°C). Our studies show that shy-B exists in two polymorphic forms. As expected from crystal chemistry, the LT polymorph crystallizes in a lower symmetry space group (*Pnn2*), whereas the HT polymorph assumes a higher symmetry space group (*Pnmm*). TEM shows that both modifications consist of nearly perfect crystals with almost no lattice defects or inclusions of additional phases. IR spectra taken on polycrystalline thin films exhibit just one symmetric OH band and 29 lattice modes for the HT polymorph in contrast to two intense but asymmetric OH stretching bands and at least 48 lattice modes for the LT sample. The IR spectra differ not only in the number of bands, but also in the response of the bands to changes in pressure. The pressure derivatives for the IR bands are higher for the HT

polymorph indicating that the high symmetry form is more compressible than the low symmetry form. Polarized, low-temperature single-crystal IR spectra indicate that in the LT-polymorph extensive ordering occurs not only at the Mg sites but also at the hydrogen sites.

Keywords Super hydrous phase B · Phase transformation · OH incorporation · Infrared · Synchrotron infrared radiation · High pressure behaviour

Introduction

Experimental studies in the system MgO-SiO₂-H₂O have demonstrated that a number of hydrous phases, the so-called dense hydrous magnesium silicates (DHMS) are stable at extremely high pressures and relatively low temperatures. If present in the Earth they could bring water within subducting slabs to depths much greater than 200 km. Members of this mineral group are the 10 Å and 3.65 Å phases and the so-called alphabet phases (e.g. A, B, superhydrous B, C, D and E). Due to their higher thermal stability shy-B and phase D are the most likely candidates to occur deep in the Earth's mantle (e.g. Frost 1999; Ohtani et al. 2003). Until recently there was considerable confusion over the nomenclature and identification of these materials: superhydrous B (shy-B) seems to be identical to phase C and phase D to phases F and G (see overviews in Prewitt and Downs 1998; Frost 1999).

Shy-B was first synthesized by Gasparik (1990) at 19 GPa and 1450°C and characterized as Mg₁₀Si₃O₁₄(OH)₄. But, although shy-B has been known for more than 10 years now, its crystal structure especially with respect to hydrogen is still under debate. The first refinement was made by Pacalo and Parise (1992) in the orthorhombic centrosymmetric space group *Pnmm* with hydrogen in just one general position (multiplicity 8) - consistent with the proposed formula (*Z* = 2).

M. Koch-Müller (✉) · R. Wirth
Department 4, Telegrafenberg, GeoForschungsZentrum
Potsdam, 14473 Potsdam, Germany
E-mail: mkoch@gfz-potsdam.de
Tel.: +49-331-288-1492
Fax: +49-331-288-1402

P. Dera · Y. Fei · Z. Liu
Geophysical Laboratory, Carnegie Institution of Washington,
5251 Broad Branch Road NW, Washington, DC 20015, USA

H. Hellwig
Department of Geology, University of Illinois
at Urbana-Champaign, Urbana, IL, 61801

J. V. Orman
Department of Geological Sciences, Case Western Reserve
University, Cleveland, OH, 44106

Hazen et al. (1997) investigated a fluorine-analog of shy-B (superflourous B) and confirmed the high symmetry space group. However, Kudoh et al. (1994) assigned a lower non-centrosymmetric symmetry of $P2_1nm$ – with hydrogen in two different general positions (multiplicity 4). This lower symmetry seems to be consistent with the existing IR- and Raman-spectra of shy-B, for example, by Cynn et al. (1996), Frost and Fei (1998), Hofmeister et al. (1999) and Liu et al. (2002), which all show two intense peaks in the OH stretching region indicating the existence of two different H sites. Thus, either one of these structure refinements is wrong or shy-B exists in two different structural modifications.

The first indication for the existence of a polymorphic phase transition in superhydrus phase B came from a comparison of the literature data: the samples, for which the higher symmetry space group was assigned, were synthesized at much higher temperatures than the ones assigned the lower symmetry space group, or for which the lower symmetry was indicated by the presence of two OH bands (Table 1).

In this study we synthesized shy-B at 22 GPa and 1200 (LT) and 1400 (HT)°C and investigated the samples by transmission electron microscopy (TEM), single crystal X-ray diffraction, Raman and infrared spectroscopy. We present proof for the existence of two polymorphs of shy-B, which come mainly from vibrational spectroscopy but are supported by single crystal X-ray diffraction.

Experimental and analytical procedure

Syntheses of shy-B were conducted in a multi-anvil apparatus at the Geophysical Laboratory. The design of the multi-anvil device is similar to that of Walker (1991), and is described in detail in Bertka and Fei (1997). The 8/3 assembly (octahedron edge length/truncated edge length) was used in all the experiments, consisting of a MgO-based octahedral pressure medium with a rhenium furnace and pyrophyllite gaskets. The temperature was measured using a W5%Re-W26%Re thermocouple and no pressure correction on the emf was applied. Both pressure and temperature were computer-controlled

Table 1 References, structure proposals and synthesis conditions of shy-B from literature

references	Structure, no of H (F) positions	OH bands ¹	synthesis conditions
Pacalo and Parise (1992)	Pnmm, 1 H	n.d.	20 GPa, 1400°C
Hazen et al. (1997)	Pnmm, 1 F	n.d.	18 GPa, 1550°C
Kudoh et al. (1994)	P2 ₁ mn, 2 H	n.d.	17 GPa, 1000°C
Cynn et al. (1996)	-	2	16 GPa, 1172°C
Frost and Fei (1998)	-	2	21 GPa, 1200°C
Liu et al. (2002)	-	2	19 GPa, 1000°C

¹no of OH bands observed in IR or Raman spectra. n.d.: no spectra were collected

during the entire duration of the runs. Welded Pt capsules with 1.18 mm outer diameter were used as sample containers. After the runs, recovered Pt-capsules were embedded in epoxy resin and ground to expose the center of the charges. Table 2 lists the starting materials, the experimental conditions, and composition of the syntheses. Initially, we synthesized shy-B for spectroscopic measurements in order to improve the assignment of the infrared bands. Therefore, in sample Jim252 about 17 mol% of the MgO was substituting by NiO and 80% of the water was added as D₂O. Thus, sample Jim252 is not of pure Mg shy-B endmember but an Mg-Ni solid solution.

For quantitative chemical analyses, the polished samples were analyzed with a JEOL JXA-8900 electron microprobe (EMP) at the Geophysical Laboratory, using synthetic oxides as standards. Operating conditions were 15 kV and 15 nA. Counting time was set at 30 s on peak and 15 s on background. Raw spectrometer data were corrected using the $\phi\rho Z$ correction procedure.

The polished samples were also used to record Raman spectra with a multichannel Raman microprobe (Dilor XY) in a backscattering configuration using a CCD detector with 1024×298 channels. The excitation source was an Argon-Ion laser operated at 514.5 nm. The laser light was focused onto the sample using a Leitz L25 objective. The typical acquisition time was 120 s with 50 mW power on the sample. Individual single crystals of both samples were checked for the presence of nanometer or submicrometer sized inclusions by TEM.

Table 2 Starting material, synthesis conditions, electron microprobe analyses and stoichiometry of Superhydrus Phase B (1 σ : standard deviation)

Starting materials	MKM-01-05 SiO ₂ , MgO, Mg(OH) ₂	Jim 252 SiO ₂ , NiO, Mg(OD,H) ₂
P (GPa)	22	22
T (°C)	1200	1400
Run duration (h)	2	4.5
Coexisting phases	Brucite	-
Wt%		
SiO ₂	30.22(26)	26.16(30)
MgO	63.49(66)	49.48(98)
NiO	-	19.54(99)
Σ	93.71(49)	95.19(51)
Cations pfu	on the basis of 16 oxygens ¹	
Si	3.12(8)	2.95(2)
Mg	9.76(16)	8.32(29)
Ni	-	1.77(18)
Σ	12.88(8)	13.05(2)
Cations pfu	on the basis of 18 oxygen ²	
Si	3.09(13)	3.01(5)
Mg	9.68(32)	8.48(20)
Ni	-	1.81(18)
H ²	4.29 (97)	3.40(37) ³

¹ Corresponding to fourteen O²⁻ and four OH⁻

² Taking the difference to 100% in the microprobe analyses as wt% H₂O

³ Assuming 80% of the water as D₂O and 20% as H₂O

Site specific TEM foils were prepared by Focused Ion Beam technique (FIB). The instrument used was a FEI FIB200 with Ga-ion source operating at 200 kV. Details of the FIB technique are given elsewhere (Overwijk and van den Heuvel 1993; Heany et al. 2001). The final thickness of the TEM foil presented here is about 120 nm. The foils are removed from the sample using a manipulator with a glass fiber under an optical microscope, and placed onto a perforated TEM carbon grid. No further carbon coating is required. TEM was performed using a Philips CM200 transition electron microscope operating at 200 kV and equipped with a LaB6 electron source. The TEM is equipped with a Gatan imaging filter GIFTM and an EDAX X-Ray spectrometer with ultrathin window. Energy filtered images were acquired by applying a 10 eV window to the zero loss peak. Electron diffraction was used to determine the orientation of the samples on which polarized single crystal IR spectra were collected.

NIR-FIR powder spectra were performed on a Bruker ISF 66 v FTIR spectrometer at the U2A beamline at the National Synchrotron Light Source, Brookhaven National Laboratory. The spectrometer was equipped with a modified IRscopeII microscope and a custom designed microscope system for far-IR measurements. Spectra were obtained on thin films in a diamond-anvil cell from ambient pressure to about 15 GPa. We used a Megabar-type diamond-anvil cell (Mao and Hemley 1998) with type II diamonds with culet sizes of about 800 μm and a stainless steel gasket. For the ambient NIR-FIR spectra, shy-B powder was placed without pressure medium on one diamond-anvil and the cell was carefully closed without pressurizing. For high-pressure measurements, thin-films of shy B were created by pressing the corresponding powdered samples in a diamond anvil cell without gasket. For the NIR-MIR range, the thicknesses of the films were calculated from interference fringes as 1.5 – 2.0 μm . The films were then embedded in the gasket hole (diameter of 100 μm) with ruby grains for the pressure measurements using CsI as a pressure medium. The aperture was set to 23×41 μm^2 and the spectra were acquired in the range of 600 - 8000 cm^{-1} with a KBr beamsplitter and a MCT detector. A resolution of 4 cm^{-1} from 512 scans was used for every spectrum. The pressure was determined from the energy shift of the R₁ ruby fluorescence line relative to its energy at ambient conditions (Mao et al. 1986). For far-IR measurements, the spectra were collected from 50 - 600 cm^{-1} with a Mylar beamsplitter and a helium cooled bolometer. The entire optical path was purged with dry N₂ during the measurements to eliminate vapor absorption. For the high-pressure measurements 20 - 25 μm thick disks of shy B were created by compressing the powdered samples in an ungasketed diamond anvil cell. Then a pre-indented stainless steel gasket with 400 μm hole in diameter was mounted on the top of one diamond anvil. The samples were embedded in the gasket hole with ruby grains for

pressure calibration and petroleum jelly as a pressure medium. The spectra were recorded with a resolution of 4 cm^{-1} from 512 scans. Aperture was set to 150×150 μm^2 .

Unpolarized single crystal spectra in the OH stretching region were recorded from ambient temperature down to -180°C on a Bruker ISF 66 v FTIR spectrometer at the GeoForschungsZentrum Potsdam, Germany with a KBr beamsplitter and a InSb detector. For the low temperature measurements we used a Linkam FTIR600 heating/cooling stage. The aperture was set to 50 – 60 μm . To avoid saturation of the detector due to strong OH absorbance polarized single crystal spectra were taken on untwinned parts of oriented crystals (TEM) with thicknesses ranging from 10 to 25 μm . They were recorded on a Nicolet 870 FTIR spectrometer equipped with a Continuum microscope at the synchrotron IR-beamline at Bessy II in Berlin, Germany, which allows an aperture size of 5×5 μm even with polarized light.

All X-ray experiments were carried out with an automated Bruker AXS P4 diffractometer equipped with a SMART 1 K CCD detector. The instrument employed graphite-monochromated MoK α radiation. The incident beam was collimated to a diameter of 0.3 mm. The sample-to-detector working distance was approximately 40 mm. The data were collected in a series of three 180° wide ω 1 scans, at χ = 0, 45 and 90°, with the CCD detector at 30° and 0.5° rotation step, and exposure time of 30 s. The data were corrected for geometrical distortion, dark current, and flood-field effects. Sample crystal orientation was determined using the Bruker SMART program. Integrated intensities were calculated using the Bruker SAINT program and were corrected for Lorentz and polarization effects. An absorption correction was applied using the SADABS program.

The structure of shy-B was solved using direct methods and the SHELXS program (Sheldrick 1997). Refinement was performed using SHELXL from the SHELXTL package (Sheldrick 1997).

To see whether the crystals are centrosymmetric or non-centrosymmetric, we applied the method of second harmonic generation (SHG). SHG describes the effect that under strong optical radiation a non-centrosymmetric material can produce output at twice the incident frequency of the incoming laser light (Nye 1985). This effect is forbidden in centrosymmetric crystals and can be detected by analyzing the light output at half the wavelength of the incoming light. The output signal scales with the square of the incoming light intensity and therefore makes the use of pulsed laser sources necessary. The setup in the present study consisted of an Nd-YAG (neodymium doped yttrium aluminium garnet) laser in q-switched pulsed mode (wavelength 1064 nm, repetition rate 6 kHz, pulse length 250 ns, average power about 400 mW). Two crystals of the HT-sample and three crystals of the LT sample were investigated. We focused the laser into the sample by using a lens with a focal length of 100 mm. The system was aligned by

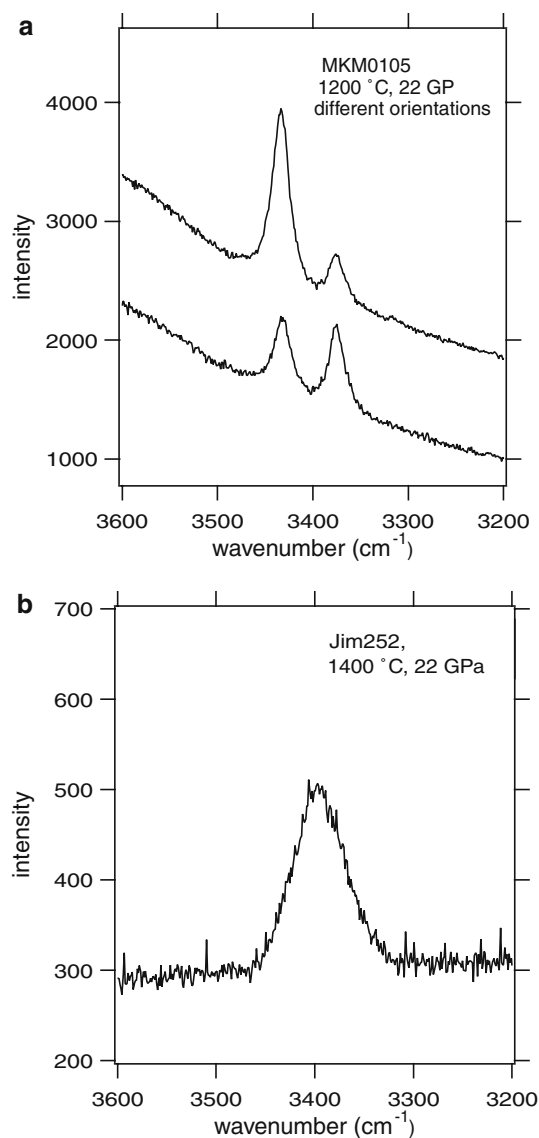


Fig. 1 Raman spectra of shy-B taken in the OH stretching range

gaining maximum intensity at the detector with a quartz sample as a reference. The transmitted light was collected, filtered through a harmonic separator and let into a monochromator in order to make sure that the spectral characteristics matched those of the second harmonic at 532 nm.

Results

Electron microprobe analyses, Raman spectroscopy, X-ray diffraction and TEM confirmed that both samples are superhydrous phase B.

According to the electron microprobe analyses the chemical formulae are $\text{Mg}_{9.76}\text{Si}_{3.12}\text{O}_{14}(\text{OH})_4$ (MKM0105) and $\text{Mg}_{8.32}\text{Ni}_{1.77}\text{Si}_{2.95}\text{O}_{14}(\text{OH},\text{D})_4$ (Jim252). Raman spectra collected in the OH stretching

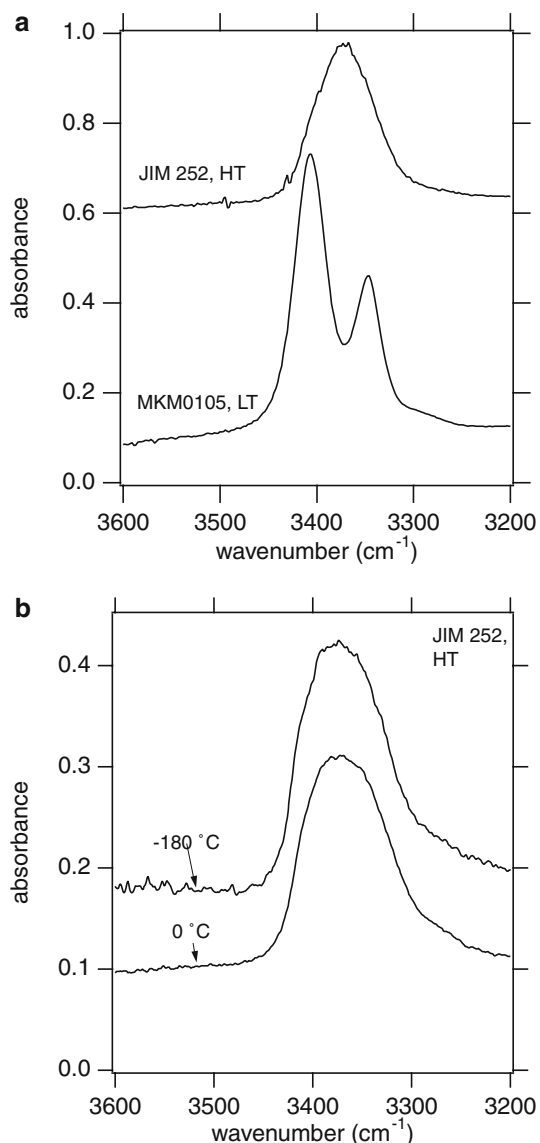


Fig. 2 Infrared spectra of shy-B taken in the OH stretching range. (a) compares the spectrum of the HT sample with that of the LT sample. (b) shows spectra of the HT sample taken at different temperatures

region on single crystal, as well as IR spectra taken in the same energy range on thin films of the samples show that the two samples differ in their number of OH bands. In both types of spectra the LT sample shows two OH stretching bands, while the spectra of the HT sample show just one relatively broad band (Figs. 1, 2). To test whether the broad band would split into two OH stretching bands, the IR spectra were taken in situ from room temperature to -180°C (Fig. 2). We observed no band splitting, which confirms that the two samples indeed differ in the number of OH bands. The higher bandwidth can be explained by the fact that sample Jim252 is a solid solution. This is the first indication that the two samples may have different structures.

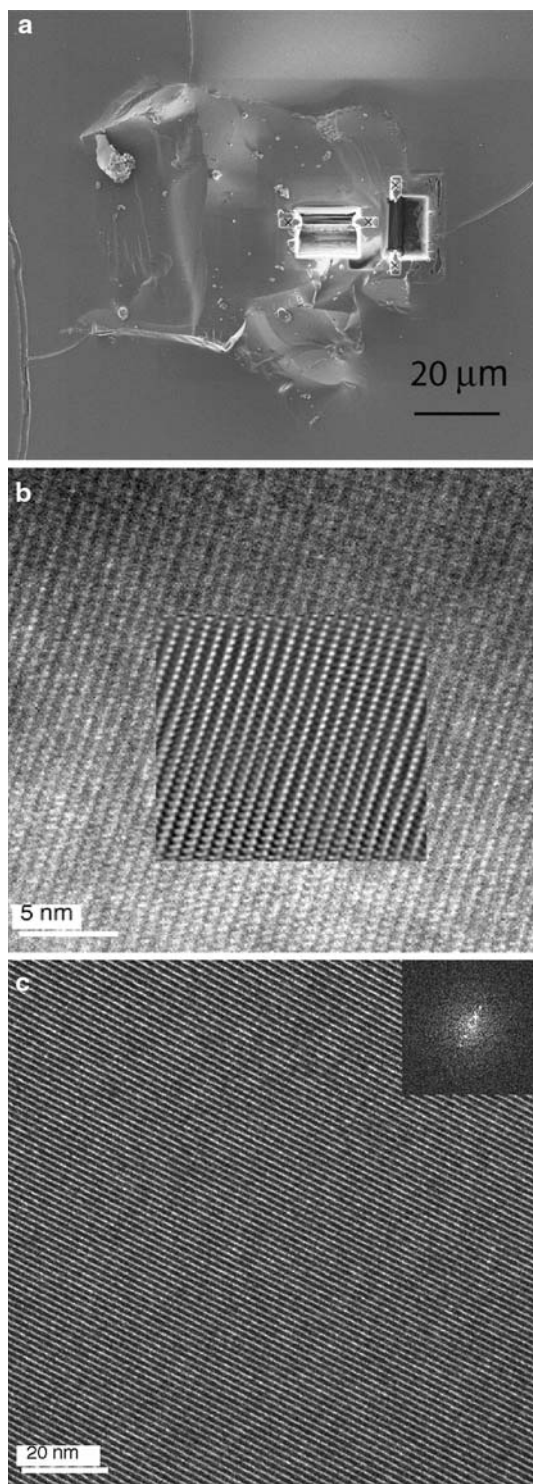


Fig. 3 (a) SE image of a crystal of the HT sample which has been investigated by TEM. The grooves where the TEM foils have been cut by the FIB technique are visible. The TEM foils are already removed. (b) and (c) energy filtered, HREM images of the HT and LT sample, respectively, with lattice fringes showing perfect crystals

Site specific TEM foils were cut from unpolished crystals mounted in crystal-bond. The secondary electron (SE) image in Fig. 3a shows the surface of a crystal

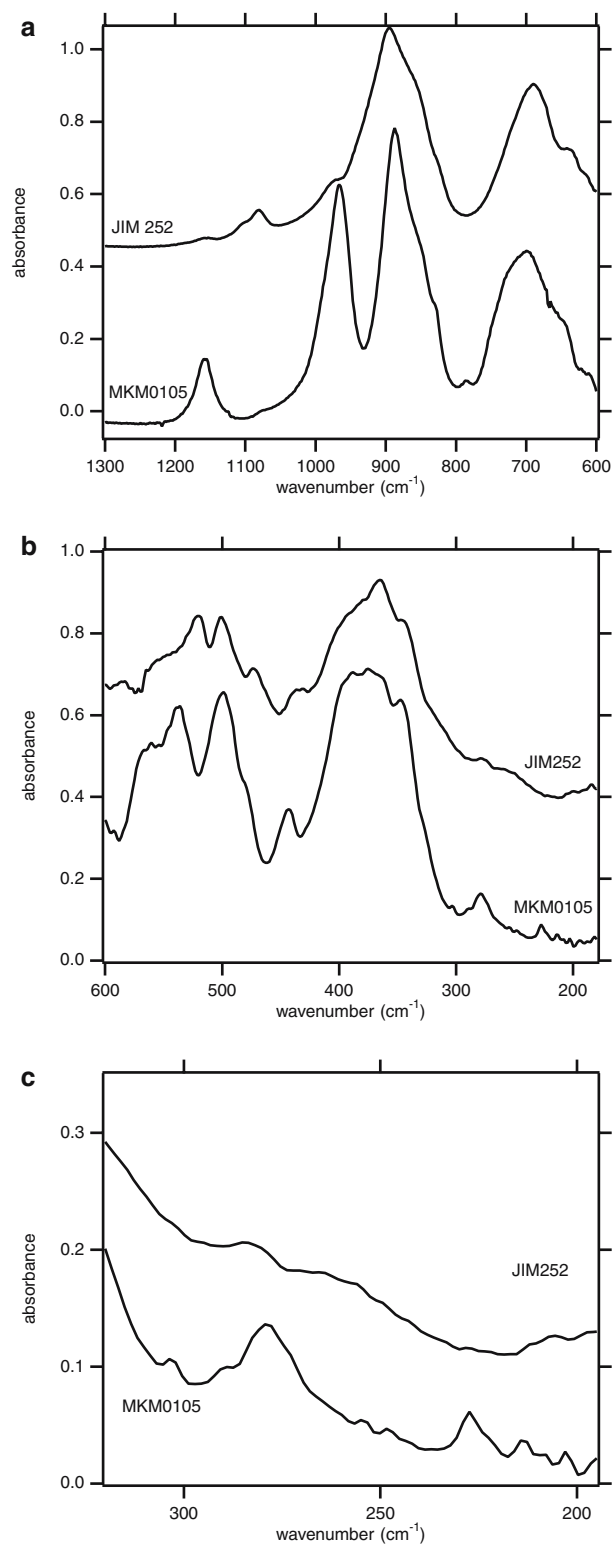


Fig. 4 MIR-FIR spectra of the LT (MKM0105) and the HT (JIM252) samples taken on thin films of similar thicknesses for the two samples

of Jim252 with the now empty grooves where the TEM foils were cut. The lattice fringe images (Fig. 3b,c) show that both samples consist of nearly perfect crystals

Table 3 Infrared bands of the LT and HT sample of shy-B and their pressure derivatives

LT-shy B			HT-shy-B			LT-shy B			HT-shy-B	
ν_{i0} (cm ⁻¹)	$\delta\nu/\delta P$ (cm ⁻¹ /GPa)	$\delta^2 \nu/\delta P^2$ (cm ⁻¹ /GPa ²)	ν_{i0} (cm ⁻¹)	$\delta\nu/\delta P$ (cm ⁻¹ /GPa)	$\delta^2 \nu/\delta P^2$ (cm ⁻¹ /GPa ²)	ν_{i0} (cm ⁻¹)	$\delta\nu/\delta P$ (cm ⁻¹ /GPa)	$\delta^2 \nu/\delta P^2$ (cm ⁻¹ /GPa ²)	ν_{i0} (cm ⁻¹)	$\delta\nu/\delta P$ (cm ⁻¹ /GPa)
3407	2.677	-0.102				547			556	1.621
3347	-0.009		3373 ^b	0.282		540				
3288 ^a	-3.631	0.141				536				
1158 ^a	6.297	-0.227	1158	3.742	-0.082	528	1.726			
1104 ^a	3.968	-0.190	1102	2.544		509	2.172		525	2.443
1072 ^a	2.233		1081	2.445		499	2.335		504	2.139
1035	2.000		1027 ^c	-0.663	0.189	492	2.347			
991	6.716	-0.281	973	2.973		479	2.377		477	2.746
966	5.527	-0.182				444	2.753	-0.055	443	3.607
950	3.776	-0.083				399	4.020	-0.090	434	2.476
915 ^a	6.410	-0.199				389	2.764		399	3.407
888	6.408	-0.307	893	4.079		374	2.857		398	3.098
857	2.075	-0.071	852	0.336	0.178	362	3.023		382	2.984
829	4.239	-0.208	826	2.858		347	3.053	-0.068	369	2.927
785	2.415		779 ^c	2.530		327	2.889	-0.079	350	2.872
750	2.262					303	1.790		319	3.023
721	6.207	-0.223	725	3.481		290	1.420		283	2.089
695	5.838	-0.192	698	2.479		279	1.877	-0.067		
669	2.948		670	1.633		273	0.432			
648	3.413		636	2.040		263	0.429		262	1.254
622	3.197					227	1.006			
610	2.343		615	3.641	-0.098	213	0.611			
580	5.656	-0.198	589	2.569		203	1.235	-0.026		
571						194	2.001	-0.061		
561						182	0.985			
554										

^a Observed at 0.6 GPa

^b Since the sample was partly deuterated an additional OD band occurs at 2507 cm⁻¹ ($\nu_{OH} / \nu_{OD} = 1.35$)

^c Observed at 1.2 GPa

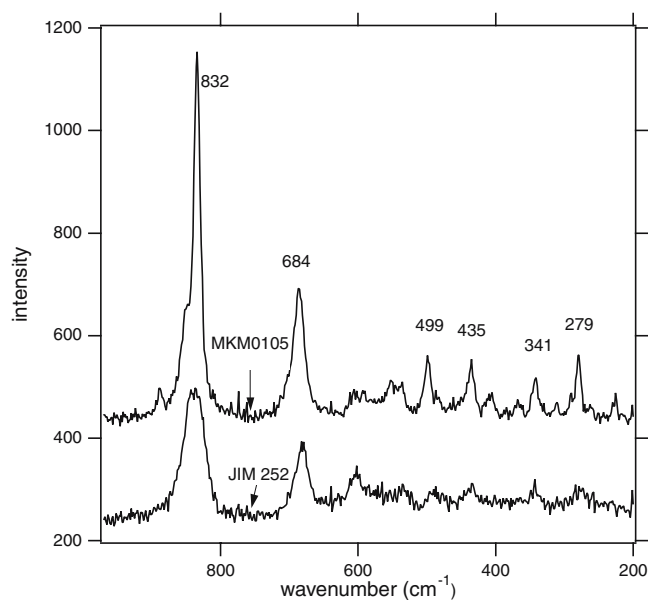


Fig. 5 Raman spectra of the LT (MKM0105) and the HT (JIM252) samples

without any inclusion of other phases. However, from the electron diffraction pattern it is not possible to distinguish between a centrosymmetric and non-centrosymmetric space group. From the electron diffraction

pattern we were able to determine the orientation of the crystals and used these crystals for the polarized single crystal IR spectroscopy. As discussed previously Pacalo and Parise (1992) proposed a centrosymmetric orthorhombic space group $Pnmm$ for shy-B with one hydrogen position. Kudoh et al. 1993 suggested a non-centrosymmetric space group $P2_1mn$ with two hydrogen positions. Taking into account that we observe one OH band in the HT sample and two in the LT sample it is evident that there is more than one crystallographically distinct variety of shy-B. But the differences between the two samples are not only related to the location and number of OH groups. Fig. 4 compares spectra in the mid and far infrared taken on polycrystalline films of the LT sample and HT sample. The HT sample shows 29 lattice modes and one OH stretching mode compared to 48 lattice modes and two OH stretching modes for the LT sample (Table 3). Raman spectra confirm the higher number of lattice modes (22) for the LT sample compared to 9 for the HT sample (Fig. 5). The IR spectra of the two samples differ not only in their number of bands, but also in the response of the bands with increasing pressure. Figure 6 shows NIR spectra, collected in situ in a DAC up to 16 GPa. The high-energy OH band of the LT sample shifts slightly to higher energies with increasing pressure, while the position of the low energy band, as well as that of the one OH band of the HT

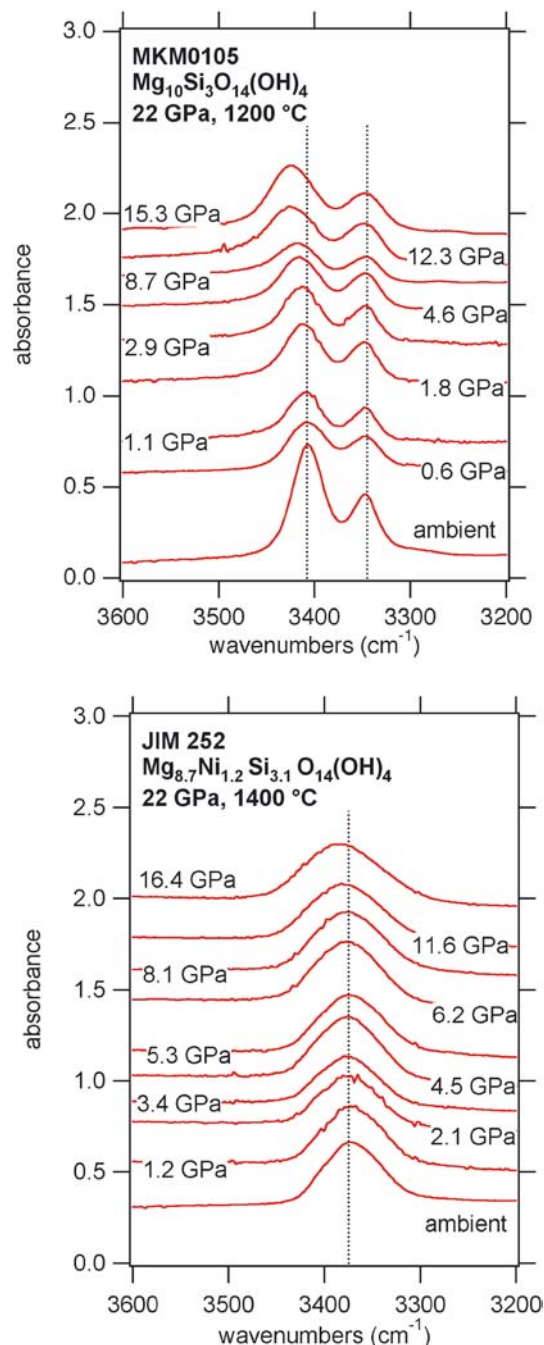


Fig. 6 NIR spectra of shy-B taken in the OH stretching region as a function of pressure

sample remain constant. The IR bands in the MIR and FIR region shift with increasing pressure to higher frequency (Figs. 7, 8 and Table 3). However, the pressure derivatives for the HT sample are higher than those for the LT sample, indicating a higher compressibility of the HT sample as compared to the LT sample. The observed difference in the compressibility could be due to the different compositions of the samples. The HT sample contains about 17 mol % Ni which is slightly smaller than Mg while the LT sample is of pure Mg shy B.

Unpolarized single crystal spectra taken in the OH stretching region on three different single crystals of the LT sample are compared in Fig. 9a with a spectrum taken on a thin film made from crystal 3. In contrast to the thin film spectrum, where two asymmetric OH bands can be observed, in the single crystal spectra more than two bands are visible. The spectra of the three crystals are different because the crystals differ in their orientation. Figure 9b shows unpolarized single crystal spectra of the LT sample as a function of temperature down to -180°C . From this it becomes clear that extensive ordering at the H sites occurs in the LT sample. The polarized single crystal IR spectra (Fig. 10a,b) indicate that two groups of bands can be distinguished, according to their polarization behavior. These two groups consist of several subsites with the same polarization behavior. Figure 10c,d shows polarized single crystal spectra in the OH stretching region taken on (100) and (010) plates of the HT sample with different settings of the polarizer. In the (100) plane the lowest intensity is observed with the electric field vector E parallel to b . In the (010) plane an isotropic polarization behavior can be observed.

The confirmation of the existence of two polymorphic space groups by single crystal X-ray diffraction was a difficult task as the refinements were complicated by extensive twinning of the crystals. It is possible to identify lack of centricity of a crystal from XRD data, if it is associated with a replacement of a glide plane or screw axis by another symmetry operation which does not cause systematic absences. In such a situation additional, weak reflection can be observed, which would be absent in a centrosymmetric case (e.g. the $Pnmm$ vs. $P2_1/mn$ case considered by Kudoh et al. 1993). It is, however, possible that the disappearance of centricity may not be accompanied by changes in systematic absences. In such a situation the judgment can be made based on the significance of the systematic-absence breaking. We have not found any evidence of systematic-absence breaking, in the collected single-crystal XRD data, and we have to rule out a space group that does not have the same systematic absence conditions. In such a case, high quality diffraction data is required, and if there is no pronounced bond geometry distortion associated with the non-centricity, the judgment about it is made on the basis of the Hamilton test (by examining the improvement in the quality of the fit, estimated by the R-factor, associated with lowering of symmetry in non-centrosymmetric group). A non-centrosymmetric subgroup will always have more independent variables describing the structure, and thus, the introduction of additional parameters in the least-squares fit may lead to a small fit quality improvement. Therefore, to support the hypothesis of the non-centricity, the improvement has to be significant enough. An obvious way of removing the centricity from the $Pnmm$ space group without affecting the systematic absences is to use the subgroup $Pnn2$. In $Pnn2$ each of the Mg-sites Mg2, Mg3, and Mg4 splits into two independent sites, thus creating

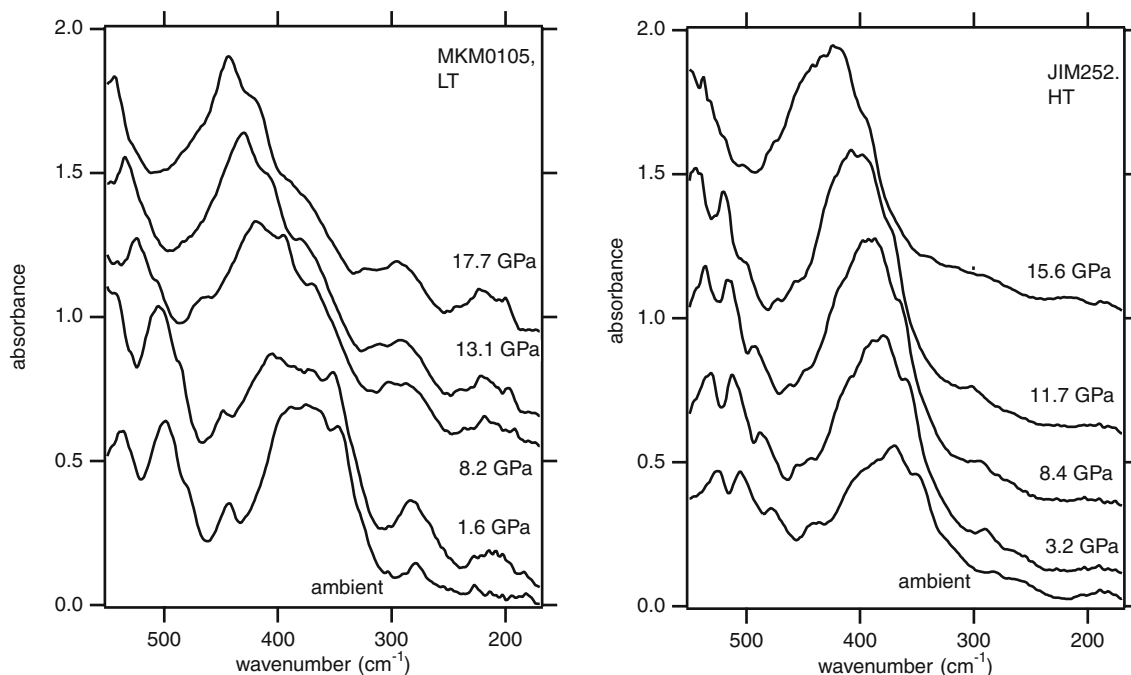


Fig. 7 FIR spectra of shy-B at different pressures

more possibilities for additional H sites. For each of the six studied crystals we performed refinements in both $Pnmm$ and $Pnn2$ space groups. For these two space groups the number of independent variables is 62 and 72, respectively. An improvement in the fit by over 1%

seems to be a strong argument for non-centricity. In all cases the refinements for sample JIM252 in space group $Pnmm$ was convincing (wR1 about 10%), and no major improvement was observed in the non-centrosymmetric space group, which is in agreement with the observation of just one OH band. On the other hand, for sample MKM0105, there was a noticeable improvement of the quality of fits in space group $Pnn2$, compared to $Pnmm$

Fig. 8 Positions of the FIR bands in shy-B as a function of pressure

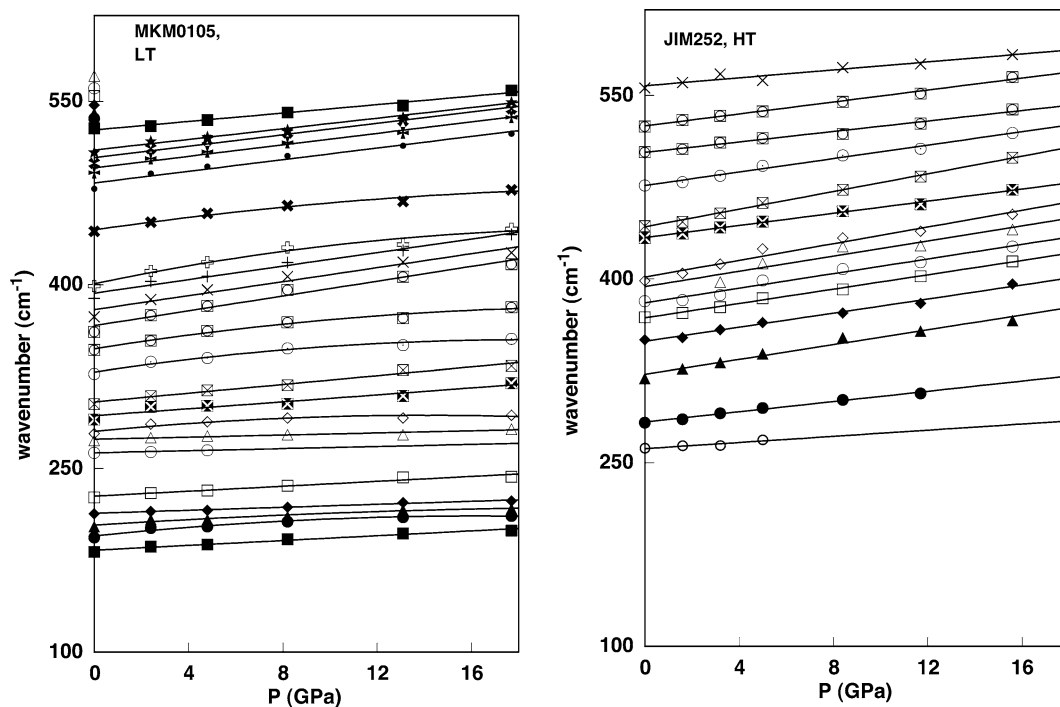
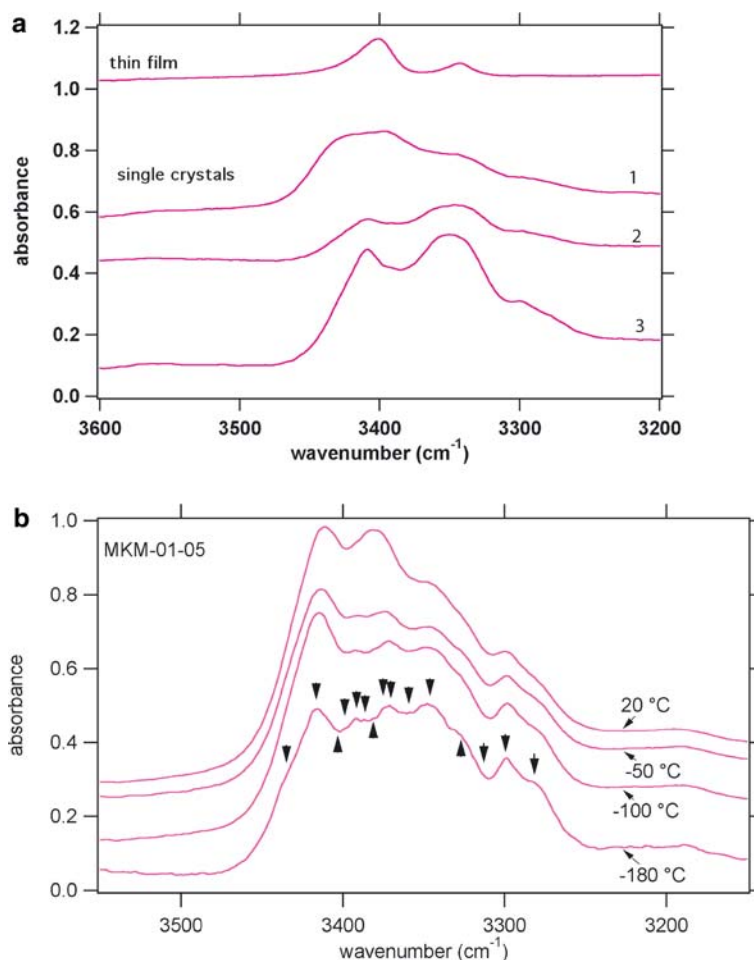


Fig. 9 (a) Unpolarized NIR spectra of three different single crystals of the LT sample in comparison to a spectrum taken on a thin film made from crystal 3. (b) Unpolarized NIR spectra of the LT samples as a function of temperature down to -180°C



(wR1 about 8% vs. wR1 about 10%). This is in agreement with the observation of two different OH bands. The comparison of the respective R-factors for two of the studied crystals is presented in Table 4 along with the fractional atomic coordinates from the refinements. Anisotropic displacement parameters (ADPs) were used for all atoms and are available from the authors upon request. In conclusion, the results of the X-ray diffraction experiments support the disordered structure model for the HT phase and an ordered structure model for the LT phase.

To confirm the results obtained by X-ray diffraction we applied the SHG method. The signal to noise ratio of the reference quartz sample was better than 100. None of the samples investigated showed significant effects in the SHG output. Unfortunately, the interaction with the laser destroyed the samples and therefore the time to obtain a signal was rather limited. While a clear SHG signal proves a non-centrosymmetric structure, a non-detectable signal might be related to a very weak effect and small sample sizes. So, with this method we neither confirm nor reject the hypothesis of the existence of a centrosymmetric or non-centrosymmetric form of shy-B.

Discussion

Single crystal X-ray diffraction analyses indicate that the HT sample crystallizes in the high-symmetry space group $Pnmm$, while the LT sample crystallizes in the low symmetry space group $Pnn2$. The vibrational spectroscopy confirms this indication. Symmetry analysis predicts 102 Raman and 82 IR modes for the high symmetry sample and 207 Raman and 155 IR modes for the low symmetry sample (Table 5). In the infrared spectra for each sample we observe about one-third of the number of bands predicted by the symmetry analyses, that is, 50 IR modes observed vs. 155 predicted for $Pnn2$ and 30 IR modes observed vs. 82 predicted for $Pnmm$. According to Cynn et al. (1996) this is what we expect for unpolarized spectra due to the degeneracy of modes in the three polarization directions. Cynn et al. (1996) report 43 lattice modes for their shy-B sample with the peak positions in good agreement with ours. We could detect in the high-pressure spectra seven more lattice modes, which overlap with other bands at ambient conditions. Raman spectra of silicates are commonly less intense than IR spectra which explains the observation of only 22 Raman lattice modes for the LT sample, in excellent

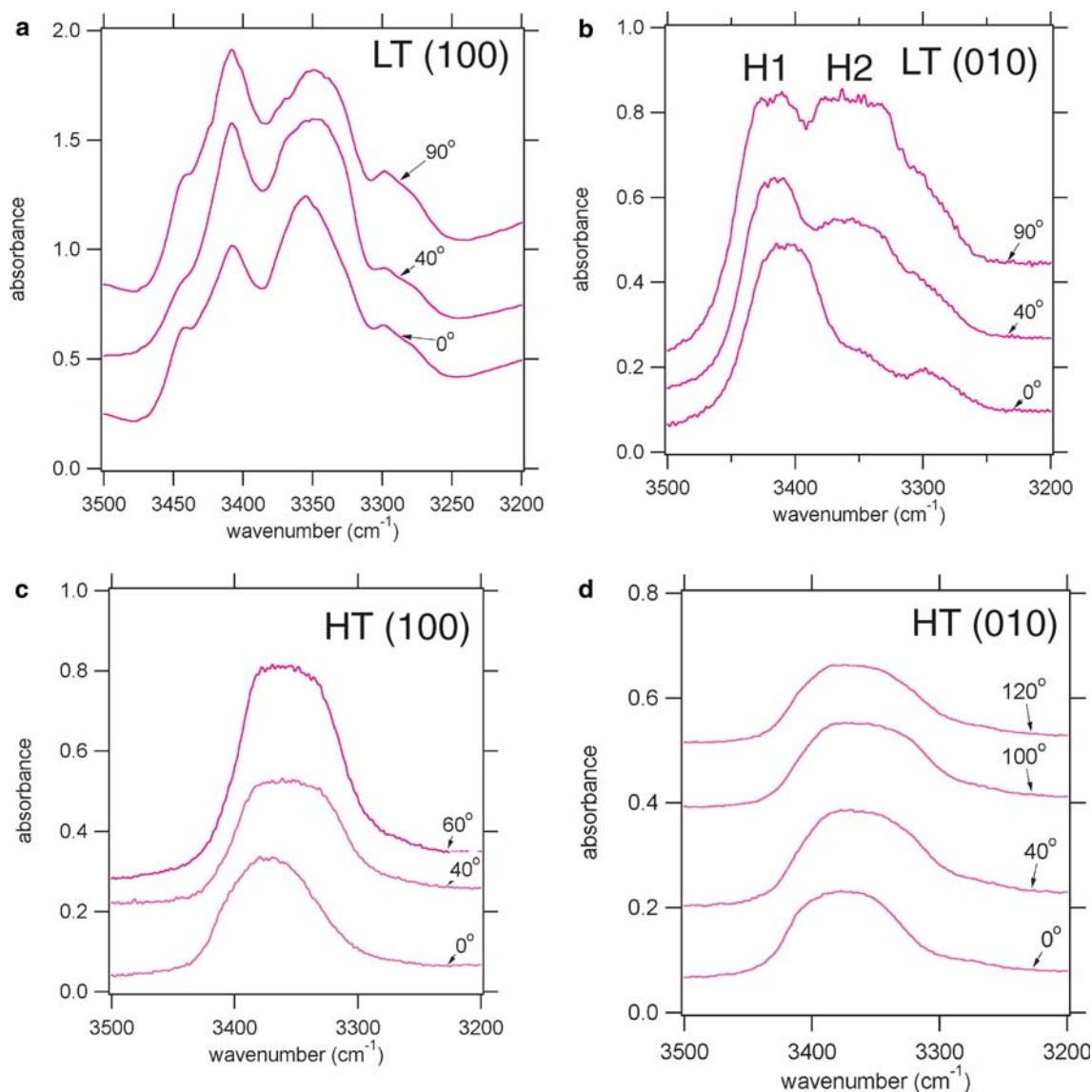


Fig. 10 (a, b) and (c, d) polarized single crystal spectra of the LT and HT samples, respectively, taken with different settings of the polarizer. The features of the OH peaks resemble those for saturated absorbance (flat top of the peak), however, we believe that this was not the case as the intensities of the single beam spectra were significantly $>$ zero within the energy range examined. Also, the features of the OH peaks are the same at relative low absorbances

agreement with Hofmeister et al. (1999), and just 9 Raman lattice modes for the HT sample. Thus, the infrared analyses confirms the existence of 2 modifications. In the low symmetry structure extensive ordering occurs on the oxygen, hydrogen and Mg sites (Table 5). Our data indicate that order/disorder depends on temperature. The disordered form occurs at higher T than the ordered which is consistent with crystal chemical observations. Whether the incorporation of Ni into our HT sample favors the crystallization of the high symmetry space group $Pnmm$ is not quite clear. Nothing is known about the effect of other

cations than Mg on the stability of superhydrous phase B. Incorporation of Ni into the structure may increase the stability of the high symmetry polymorph to lower temperatures and thus stabilize superhydrous phase B in a wider P,T field than previously expected.

Kudoh et al. 1994 suggested space group $P2_1mn$ for shy-B. In space group $P2_1mn$ not only is the H site split into two but also the tetrahedral Si site. However, this is contrary to results obtained by NMR spectroscopy. Phillips et al. (1997) collected ^{29}Si and ^1H NMR spectra of the same sample which was investigated by Cynn et al. (1996) showing two OH bands. The ^1H NMR spectra confirm the presence of two different hydroxyl groups. But they observed just one Si^{IV} peak. Two H sites and just one Si^{IV} site is in perfect agreement with space group $Pnn2$ (Table 5).

Pacalo and Parise (1992) refined the crystal structure of shy-B, synthesized at 1400°C and 20 GPa in space group $Pnmm$. In this centrosymmetric space group one H position (multiplicity 8) is enough to account for the 4 OH in

Table 4 Representative crystal data and structure refinement results for shy-B in space group Pnn2 and Pnnm.

	MKM0105			JIM252		
	<i>Pnn2</i>	<i>Pnnm</i>		<i>Pnn2</i>	<i>Pnnm</i>	
final R_1 for $I > 3 \sigma$	8.36	10.21		7.42	7.94	
final R_1 for $I > 3 \sigma$	13.18	14.32		10.92	10.70	
final R_1 for all	14.47	16.61		13.08	14.32	
final wR_2 for all	16.56	18.28		14.29	15.23	
Space group	<i>Pnn2</i>			<i>Pnnm</i>		
a (Å)	14.024(21)			13.991(2)		
b (Å)	5.109(4)			5.097(1)		
c (Å)	8.733(12)			8.715(1)		
	atomic coordinates (x 10 ⁴)			atomic coordinates (x 10 ⁴)		
	<i>X</i>	<i>Y</i>	<i>Z</i>	<i>X</i>	<i>Y</i>	<i>Z</i>
Si(1)	0	0	10077(13)	0	0	0
Si(2)	3766(2)	141(7)	51(9)	3765(1)	144(4)	0
Mg(1)	1731(3)	3279(9)	53(12)	1729(1)	3301(4)	0
Mg(21)	1775(5)	8358(17)	1752(9)	1758(1)	-1590(3)	1756(2)
Mg(22)	3240(4)	3461(14)	3242(6)			
Mg(31)	0	5000	8286(12)	0	0	3413(2)
Mg(32)	0	5000	1870(11)			
Mg(41)	0	0	6625(10)	0	5000	1776(2)
Mg(42)	0	0	3455(13)			
O(1)	4153(5)	7088(17)	-64(18)	2519(3)	5149(8)	1579(5)
O(2)	783(5)	6931(17)	50(20)	4152(4)	-2897(11)	0
O(31)	2495(8)	220(30)	3451(14)	787(4)	6993(11)	0
O(32)	2552(11)	5120(30)	1620(20)			
O(41)	760(10)	1440(30)	1531(17)	731(3)	1428(7)	1452(4)
O(42)	4298(8)	6470(30)	3619(14)			
O(51)	4145(9)	1530(30)	1599(16)	4134(3)	1672(7)	1555(4)
O(52)	889(8)	6850(30)	3479(14)			
O(6)	2598(5)	48(19)	3479(14)	2577(4)	51(12)	0
H(1) ^a	3000	6000	1000	3000	6000	1000
H(2) ^b	2700	1800	4500			

^aFrom structure refinement ^bConcluded from polarized single crystal IR spectroscopy $R_1 = \frac{\sum_{hkl} ||F_{\text{obs}}(hkl)| - |F_{\text{calc}}(hkl)||}{\sum_{hkl} |F_{\text{obs}}(hkl)|}$ $wR_2 = \frac{\sum_{hkl} w(F_{\text{obs}}^2(hkl) - F_{\text{calc}}^2(hkl))^2}{\sum_{hkl} w(F_{\text{obs}}(hkl))^4}$

the formula unit ($Z = 2$). The H position was located using a Fourier difference map. The refined fractional coordinates are -0.0769 (x), 0.3026 (y), and 0.1085 (z). These are in good agreement with our proposal (Table 4, but note

the different setting). Figure 11 shows the orientation of the OH dipole of shy-B in structure Pnnm. The observed polarization behavior of the OH bands (Fig. 10) is in

Table 5 Symmetry analysis and site multiplicity for space groups *Pnnm* and *Pnn2*

	<i>Pnnm</i>		<i>Pnn2</i>
Raman active modes	$27 A_g + 27 B_{1g} + 24 B_{2g} + 24 B_{2g}$	Raman active modes	$52 A_2$
IR active modes	$22 B_{1u} + 30 B_{2u} + 30 B_{3u}$	IR and Raman active modes	$51 A_1 + 52 B_1 + 52 B_2$
Total no of modes	102 Raman and 82 IR modes, including 1 OH stretching mode	Total no of modes	207 Raman and 155 IR modes, including 2 OH stretching modes
Site multiplicity			
Si1 ^[4]	2	Si1 ^[4]	2
Si2 ^[6]	4	Si2 ^[6]	4
Mg1	4	Mg1	4
Mg2	8	Mg21	4
		Mg22	4
Mg3	4	Mg31	2
		Mg32	2
Mg4	4	Mg41	2
		Mg42	2
H	8	H1	4
		H2	4
	6 different O sites		9 different O sites

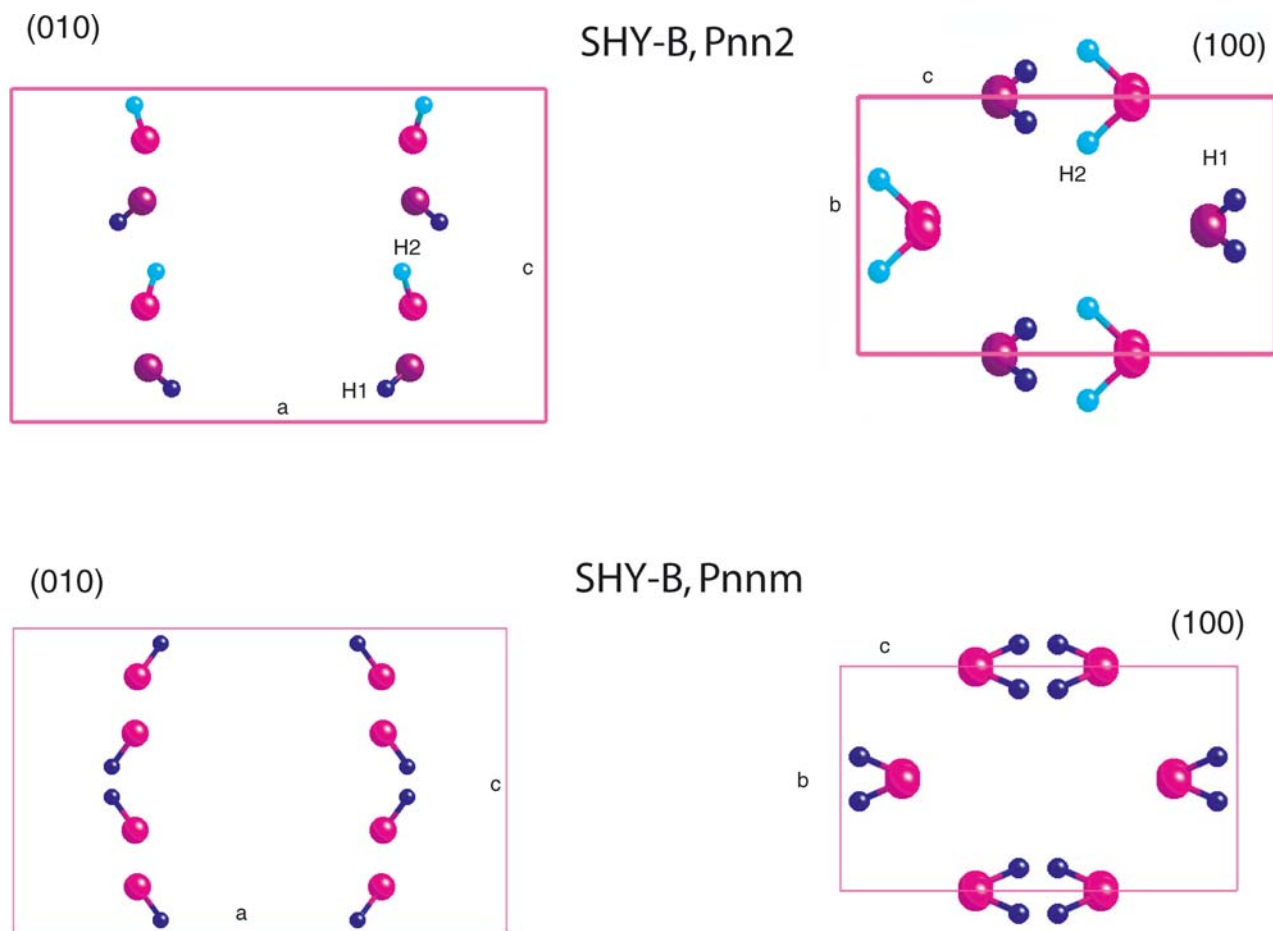


Fig. 11 Projections of the proposed orientations of the OH dipoles in shy-B of symmetry $Pnn2$ (LT sample) and shy B of symmetry $Pnmm$ (HT sample) on (010) and (100) planes

good agreement with the OH dipole directions as proposed by Pacalo and Parise (1992) and confirmed by us.

By analogy with the high symmetry form we propose for the LT sample two different OH dipoles (Fig. 11). The orientations of the dipoles are in accordance with the polarization behavior of the OH bands (Fig. 10). In the (100) plane for both OH groups an isotropic polarization behavior can be observed. In the (010) plane the same is true for the OH1 group but a strong anisotropic behavior is observed for the OH2 group with the highest intensity with the electric field vector parallel to c . The fractional atomic coordinates in space group $Pnn2$ are given in Table 4.

Conclusions

Superhydrous phase B exists in at least two modifications: a disordered high-temperature polymorph and an ordered low-temperature polymorph. The high-temperature polymorph seems to be more compressible than the

low-temperature form. In the low-temperature polymorph extensive ordering occurs not only at the Mg-sites but also at the hydrogen sites. It seems that cation order/disorder and/or partitioning of other cations into shy-B could stabilize superhydrous phase B in a wider P,T field than previously expected.

Acknowledgments We thank C. Hadidiacos for the help with the electron microprobe analyses, B. Mysen and J. Schicks for access and help with the Raman spectrometer and U. Schade for support at the synchrotron beamline Bessy II. D. Rodny is thanked for preparation and IR measurements. C.T. Prewitt is thanked for helpful comments and discussions. The comments and suggestions by Dan Frost and an anonymous reviewer helped to improve the manuscript.

References

- Bertka CM, Fei Y (1997) Mineralogy of the Martian interior up to core-mantle boundary pressures. *J Geophys Res* 102:5251–5264
- Cynn H, Hofmeister AM, Burnley PC, Navrotsky A (1996) Thermodynamic properties and hydrogen speciation from vibrational spectra of dense hydrous magnesium silicates. *Phys Chem Miner* 23:361–376
- Frost DJ (1999) The stability of dense hydrous magnesium silicates in Earth's transition zone and lower mantle. In: Fei Y, Bertka CM, Mysen BO (eds) *Mantle Petrology: Field Observations and High Pressure Experimentation: A Tribute to Francis R. (Joe) Boyd*. The Geochemical Society, pp 283–296

- Frost DJ, Fei Y (1998) Stability of phase D at high pressure and high temperature. *J Geophys Res* 103:7463–7474
- Gasparik T (1990) Phase relations in the transition zone. *J Geophys Res* 95:15751–15769
- Hazen RM, Yang H, Prewitt CT, Gasparik T (1997) Crystal chemistry of superfluorous phase B ($Mg_{10}Si_3O_{14}F_4$): implications for the role of fluorine in the mantle. *Am Mineral* 82:647–650
- Heaney EP, Vicenzi EP, Giannuzzi LA, Livi KJT (2001) Focused ion beam milling: a method of site-specific sample extraction for microanalysis of Earth and planetary materials. *Am Mineral* 86:1094–1099
- Hofmeister AM, Cynn H, Burnley PC, Meade C (1999) Vibrational spectra of dense, hydrous magnesium silicates at high pressure: Importance of the hydrogen bond angle. *Am Mineral* 84:454–464
- Kudoh Y, Nagase T, Ohta S, Sasaki S, Kanzaki M, Tanaka M (1994) Crystal structure and compressibility of superhydrous phase B, $Mg_{20}Si_6H_8O_{36}$. In: Schmidt SC, Shaner JW, Samara GA, Ross M (eds) *High-Pressure Science and Technology*, pp 469–472
- Liu LG, Lin CC, Mernagh TP, Inoue T (2002) Raman spectra of phase C (superhydrous phase B) at various pressures and temperatures. *Eur J Mineral* 14:15–23
- Mao HK, Hemley RJ (1998) New windows on the earth's deep interior. In: Hemley RJ (ed): *Ultra-high-Pressure Mineralogy*. Review in *Mineralogy* 37:1–32
- Mao HK, Xu J, Bell PM (1986) Calibration of the Ruby pressure gauge to 800 kbar under quasi-hydrostatic conditions. *J Geophys Res* 91:4673–4676
- Nye JF (1985) *Physical properties of crystals*. Clarendon Press, Oxford
- Ohtani E, Toma M, Kubo T, Kondo T, Kikegawa T (2003) In situ X-ray observation of decomposition of superhydrous phase B at high pressure and temperature. *Geophys Res Lett* 30:1029–1032
- Overwijk MHF, van den Heuvel FC (1993) Novel scheme for the preparation of transmission electron microscopy specimens with a focused ion beam. *J Vac Science Tech B* 11:2021–2024
- Pacalo REG, Parise JB (1992) Crystal structure of superhydrous B, a hydrous magnesium silicate synthesized at 1400°C and 20 GPa. *Am Mineral* 77:681–684
- Phillips BL, Burnley PC, Worminghaus K, Navrotsky A (1997) ^{29}Si and 1H NMR spectroscopy of high-pressure hydrous magnesium silicates. *Phys Chem Minerals* 24:179–190
- Prewitt CT, Downs RT (1998) *High-Pressure Crystal Chemistry*. In: Hemley RJ (ed): *Ultra-high-Pressure Mineralogy*. Review in *Mineralogy* 37:284–317
- Sheldrick G (1997) SHELXTL. Bruker AXS
- Walker D (1991) Lubrication, gasketing, and precision in multianvil experiments. *Am Mineral* 76:1092–1100